Biointerphases (2012) 7:35
DOI 10.1007/s13758-012-0035-9

ARTICLE

Contactless Laser-Assisted Patterning of Surfaces for Bio-Adhesive Microarrays

H. Perez-Hernandez · T. Paumer · T. Pompe · C. Werner · A. F. Lasagni

Received: 28 March 2012 / Accepted: 24 April 2012 / Published online: 15 May 2012

Abstract Micropatterned surfaces with cell adhesive areas, delimited by protein repellent microstructures, are in high demand for its potential use as relevant biological assays. This is not only because such surfaces allow directing cell growth in a spatially localized and restricted manner, but also because they can be used to elucidate basic cell growth and orientation mechanisms. Here, it is presented a laser-assisted micropatterning technique to fabricate large area microstructures of poly (ethylene glycol) hydrogel onto a cell adhesive surface: a biofunctional maleic anhydride copolymer. By varying photoinitiator, laser intensity, copolymer as well as the hydrogel layer thickness, the optimum conditions to produce high quality features were found. The suitability of these micropatterned substrates for bioassay applications was proved by cell adhesion studies. The introduced procedure could be used to prepare a broad range of microarrays for certain bioanalytical approaches and to create different types of biofunctional surfaces.

H. Perez-Hernandez · A. F. Lasagni (✉)
Fraunhofer Institut für Werkstoff -und Strahltechnik (IWS), Winterbergstraße 28, 01277 Dresden, Germany
e-mail: andres-fabian.lasagni@iws.fraunhofer.de

H. Perez-Hernandez
Institute for Laser and Surface Technology, Technical University of Dresden, 01062 Dresden, Germany

T. Paumer · T. Pompe · C. Werner
Leibniz Institute of Polymer Research, Max Bergmann Center of Biomaterials, Hohe Straße 6, 01069 Dresden, Germany

C. Werner
Center for Regenerative Therapies Dresden, 01307 Dresden, Germany

1 Introduction

There are still many challenges to be addressed in surface engineering for cell growth applications. The manufacturing of patterned surfaces with well-defined protein adhesive microdomains through faster methods and commercially available materials is one of them. Such surfaces are relevant for the fabrication of biological high-throughput screening assays for a wide range of applications ranging from biochips to tissue engineering [1]. Even though certain progress have been made on the manufacturing of 3D structures and performing cell culture therein, most of the in vitro bioassays are still 2D due to the wealth of 2D analytical techniques available [2–5]. In order to gain meaningful insights in the processes of cell proliferation, differentiation as well as cell-surface interactions, a variety of 2D multimaterial engineered surfaces have been developed, so that suppressing non-specific adsorption in certain regions, cell orientation and growth can be studied [6–9]. In such approaches, cell adhesion is controlled by incorporating certain moieties that favour biocompatibility while minimizing adsorption of other biomolecules present in the cell growth media [10–13]. These engineered surfaces are relevant to elucidate the factors that control cell-surface interactions [2, 14–16].

Poly(ethylene glycol) diacrylate (PEGDA) in the presence of a photoinitiator and upon UV light exposure, can undergo readily crosslinking by a free radical mechanism to form a loosely interconnected network [17]. This photocrosslinking reaction can take place at mild conditions and can be carried out even in the presence of biological fluids [18]. Furthermore, PEGDA hydrogels have the ability to swell and retain a high water content, are biocompatible and mechanically very similar in behaviour to soft tissue. Another interesting aspect of these materials is their protein-repellent property which makes PEGDA microstructures a very effective barrier

material to confine cells in certain predetermined regions or positions. Regular and well-defined hydrogel micropatterns have proved to be a useful tool to elucidate basic cell spatial behaviour and to perform semi-quantitative studies [16, 19]. Since conclusive bioassays require a large number of micropatterned probes for sequential studies, it is necessary to find a medium scale production method to fabricate such micropatterns in a cost effective and fast way.

There are several approaches to fabricate bioadhesive domains on or around protein repellent PEGDA microstructures. One of them, a modified soft lithographic technique, consists on changing certain areas of the PEG hydrogel surface to become cell adhesive, as it has been previously reported [20, 21]. In such procedures, mechanical compliance and swelling of the substrate limits the resolution of the micropatterns, and makes difficult to obtain good quality features. Also these adhesive microdomains can lose their characteristics over time because cell secretions change the areas of chemical modification as well as the surface itself [21]. Other techniques like photolytography [1, 22], laser printing [22], and direct laser writing [23] have several processing steps or require long processing times to pattern large area samples.

Microcontact printing and soft lithography have also been used to produce micropatterned surfaces with PEG hydrogels. However, techniques that require a stamp have certain inherent limitations. One of these limitations is lateral diffusion that has been observed on stamps inked with PEG hydrogel [24], that makes difficult to obtain well defined hydrogel free areas. Thus, fast homogenous micropatterning of large areas is rather limited.

Here, it is presented an alternative laser-assisted contactless micropatterning method which uses a micro lens arrays (MLA) to photocrosslink poly(ethylene glycol) dimethacrylate (PEGDMA) hydrogel microstructures onto different functional polymer surfaces for biological applications. Depending on the type of MLA used, different regular micropatterns (dots, crosses or lines) were fabricated. By successive microtranslation of the sample, micropatterns with different spatial periods and geometries were also obtained. The effect of laser processing parameters as well as pre- and post-processing on the quality of the micropatterns was investigated. Finally, laterally restricted adsorption of model proteins (albumin and fibronectin) combined with cell adhesion experiments were used to demonstrate the viability of the proposed method.

2 Materials and Methods

2.1 Sample Preparation

Glass coverslips coated with poly(octadecene-*alt*-maleic anhydride) (POMA), poly(ethene-*alt*-maleic anhydride) (PEMA), poly(propene-*alt*-maleic anhydride) (PPMA), hydrolyzed poly(styrene-alt-maleic anhydride) (PSMA-h) prepared as previously described elsewhere [13]. PEGDMA MW 600 (Sartomer), 2-hydroxy-1-[4-(2-hydroxyethoxy)phenyl]-2-methyl-1-propane (Irgacure 2959, BASF), and DL-camphorquinone (Polysciences) were used as supplied, kept and handled in a UV light free area.

2.2 Micro Lens Array Patterning

For the micropatterning process, glass coverslips prepared with a thin film of one of the four different maleic anhydride copolymers were coated with a layer of the photoreactive mixture with thickness from 125 to 300 μm, with either 5 % w/w of DL-camphorquinone or 0.1–5.0 % w/w of 2-hydroxy-1-[4-(2-hydroxyethoxy) phenyl]-2-methyl-1-propane (HHEPMP) in PEGDMA 600, which was applied by manual drawdown. After this, the samples were irradiated using a 10 ns pulsed Nd:YAG laser (Quanta-Ray PRO 290, Spectra Physics) at 355 nm through a cylindrical (for a linear pattern with a pitch of 300 μm) or spherical (for dot arrays with a pitch of 150 μm) fused silica MLA from SuSS Micro Optics. To make linear patterns with different geometries (e.g. to produce a smaller spatial period or cross patterns using the cylindrical MLA), the substrate was translated horizontally or rotated and the samples were reirradiated. To improve physisorption of the PEG hydrogel microstructures onto the surface of the substrate, the samples were briefly heated on a hot plate at 80 °C (heating time needed was shorter or longer depending on the copolymer of the prelayer used). Then, the samples were allowed to cool down for about 1 min at room temperature. Finally, the excess of no crosslinked PEGDMA was rinsed in deionized water and allowed to dry at room temperature. The schematic description of the process is given in Fig. 1.

2.3 Protein Adsorption and Cell Culture Tests

Protein adsorption and later cell culture tests were performed similarly to procedures described recently [25]. The samples were immersed in 70 % v/v of ethanol/water to provide sterile conditions for cell culture. Next, the polymer surfaces were immersed in a 50 μg/ml rhodamine-labelled bovine serum albumin (BSA) (Invitrogen, Karlsruhe, Germany) or fibronectin (purified from human plasma) solution in phosphate buffered saline (PBS) (Sigma) at pH 7.4 and 37 °C for 1 h. Carboxytetramethylrhodamine FluoReporter (Invitrogen, Karlsruhe, Germany) was used to label fibronectin prior to the experiments.

Human endothelial cells from umbilical cord vein (HUVECs) were seeded in endothelial cell growth medium ECGM (Promocell, Heidelberg, Germany) containing 2 %

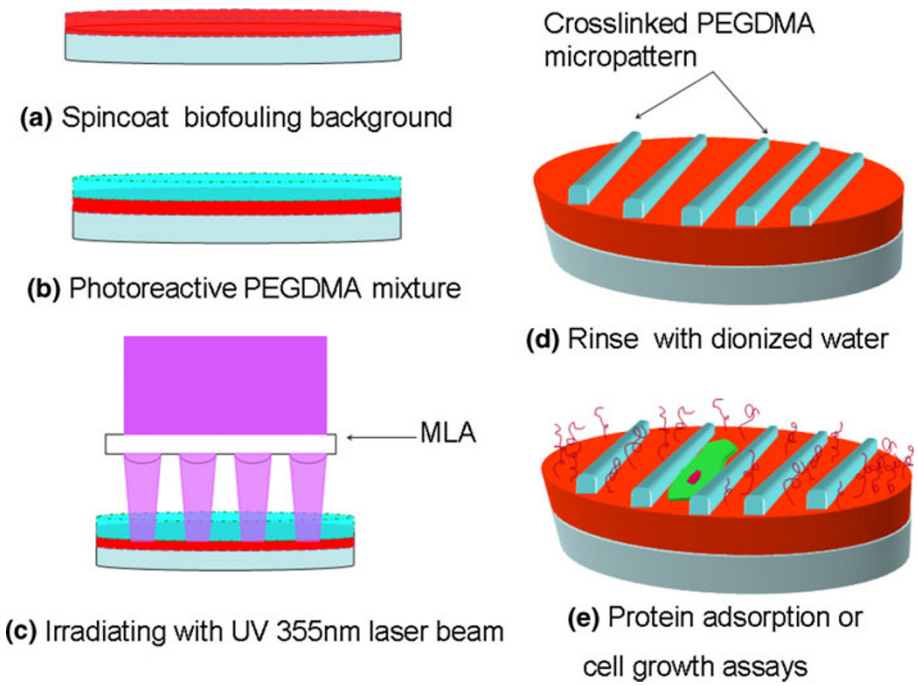

Fig. 1 Schematic representation of the procedure to make micropatterns using a micro lens array

fetal calf serum at a density of 2–10 $\times$ 10^4 cells/cm^2 on the fibronectin-coated substrates. After 3 h or 5 days of cell culture, samples were fixed with 4 % paraformaldehyde for 10 min and stained with DAPI (Sigma) and phalloidin-Alexa 488 (Invitrogen) to stain nuclei and actin cytoskeleton, respectively. The microscopic analysis were performed on inverse confocal laser scanning microscope (ICLSM, model SP5, Leica Microsystems, Germany) with a 20 or 40 x oil-immersion objectives. The width of PEG hydrogel microstructures was measured in swollen state from fluorescence microscopic pictures on microarrays after rhodamine-labelled BSA adsorption with ICLSM. In dry state, the width of the micropatterns was measured using a scanning electron microscopy (SEM) at an operating voltage of 5 kV (Philips XL30 ESEM-FEG).

3 Results and Discussion

Several of the parameters that affect the micro lens array patterning (MLAP) procedure were investigated. Four different biofunctional copolymers (POMA, PSMA-h, PPMA and PEMA), each with different degree of hydrophilicity [26], were tested as biofunctional prelayers for MLAP of PEGDMA. Polymerized hydrogel microstructures showed good to fair adhesion depending on the copolymer prelayer used. It was observed that the uniformity and quality of the photocrosslinked PEGDMA improved significantly as hydrophilicity of the prelayer increased (see Table 1). After photocrosslinking, the micropatterned surfaces were briefly heated on a hot plate to improve adhesion. The adhesion of the hydrogel structures was qualitatively proved in wet (swollen condition) by their resistance to detachment when flushed with water. Heating times (varied from 0.5 to 2 min) and temperatures (changed from 60 to 90 °C) that were found adequate for each of the different prelayers are also listed in Table 1. On the most hydrophobic prelayer (POMA with a contact angle of 100°) [26], strong dewetting of the reactive mixture and poor adhesion of the microstructures was observed. Hydrogel stripes onto POMA coated surfaces exhibited weak adhesion even after long heating following irradiation. The best physisorption and pattern resolution was observed on PEMA coated surfaces, which present the highest hydrophilicity (with a contact angle of $\sim$57°). The good adhesion of the hydrogel micropatterns on PEMA probably arises from a combination of optimal physisorption and even wetting of the liquid photoreactive mixture that allows a uniform spreading of the mixture over the surface before irradiation.

Adhesion of the photocrosslinked hydrogel by physisorption can occur during the irradiation process by to two different main effects. First, excess free radicals from the photocrosslinking reaction of the PEGDMA can promote interaction of the evolving hydrogel network with the underlying copolymer layer and improve adhesion. Second, adhesion can also be promoted by the presence of polar groups in the prelayer copolymer. In the case of the selected maleic anhydride copolymers used as prelayers, the presence of additional polar groups in PEMA and PPMA copolymers can explain the better adhesion of the hydrogel microstructures. On the other hand, when the maleic

Table 1 Summary of the effect of the biofunctional polymer pre-coating and thermal treatment of the sample on pattern adhesion and resolution

Photoinitiator (% w/w)	Biofunctional polymer precoating (water contact angle)	Pre-thermal treatment time (s) at 80 °C (before irradiation)	Post irradiation thermal treatment time at 80 °C (s)	Cooling time at room temperature (s)	Adhesion	Resolution
DL-camp (5)	PEMA (57°)	30	90	120	+	++
DL-camp (5)	PPMA (52°)	30	90	120	+	+
DL-camp (5)	POMA (100°)	30	90	120	−	−
Irgacure 2959 (0.1)	PEMA (57°)	Not necessary	40	Not necessary	++	++
Irgacure 2959 (0.1)	PSMA-h (75°)	Not necessary	60	Not necessary	+	++

anhydride copolymers have longer or bulkier hydrophobic groups (PSMA and POMA), the anhydride groups have less interactions with the highly hydrophilic PEG hydrogel polymer network of the microstructures, since there are less polar groups available to interact by hydrogen bonding, Van der Waals or other physical interfacial forces. Therefore, hydrogel structures on more hydrophilic prelayers have better adhesion due to good physisorption and interfacial interaction with the substrate. Hence, if only few polar groups are available to form hydrogen bonds, as in the case of the POMA copolymer the more hydrophobic prelayer, then poor adhesion is observed.

Two photoinitiators were used to photocrosslink PEGDMA: HHEPMP and DL-camphorquinone. The sensitivity of each photoinitiator at 355 nm can be directly correlated to their respective absorptivity at this wavelength, which affects the exposure dose (energy density given by the product between pulse energy per unit of area, or laser fluence, and the number of used laser pulses) of laser light required to crosslink PEGDMA hydrogel. Furthermore, as the photocrosslinking reaction occurs in air, the optimum photoinitiator concentration has to compensate for the free radicals that are lost by oxygen quenching but still be enough to control the polymerization rate.

For the combination of PEGDMA and DL-camphorquinone, crosslinking could be achieved at 5 % w/w of photoinitiator when irradiating at 355 nm only at relative high laser fluences (>130 mJ/cm^2) and using a large number of laser pulses (>80), see Fig. 2a. This is due to the moderate absorbance of DL-camphorquinone at this wavelength. Photocrosslinking of this mixture with lower quantities (1 and 3 % w/w) of DL-camphorquinone was not observed, even when using more laser pulses (>80 pulses) and higher laser intensities.

The total exposure dose required to initiate photocrosslinking using DL-camphorquinone was approximately 14.0 ± 0.8 J/cm^2 (lower short-dashed line in Fig. 2a). In this case, the obtained structures were very thin (~4–6 μm wide in swollen state) and most of them detached easily when rinsing the sample. Furthermore, as depicted in Fig. 2a by the solid line, there is a range of conditions to prepare mechanically stable and well-defined micropatterns (with a total exposure dose of 17.7 ± 1.7 J/cm^2). On the other hand, at the upper photocrosslinking limit (exposure doses larger than 19.5 ± 2.6 J/cm^2), the PEGDMA structures were either too wide or too tall, presenting low resolution or low mechanical stability, thus collapsing. Also some evaporation of the PEGDMA was observed in this case. Moreover, for irradiation conditions with exposure doses over the optimum (solid line in Fig. 2a), the microstructures were not distinguishable since PEGDMA was also polymerized between the lines. In consequence, these conditions were not further used in this work (upper dashed line in Fig. 2a).

In addition to DL-camphorquinone, 2-hydroxy-1-[4-(2-hydroxyethoxy) phenyl]-2-methyl-1-propane (HHEPMP, Irgacure 2959) was also used as photoinitiator. Using HHEPMP, photocrosslinking was achieved with fewer pulses as well as much lower laser fluences (from 29 mJ/cm^2 with 40 pulses for 0.1 % of HHEPMP, see Fig. 2b). The total exposure dose for this mixture was much lower (~1.18 J/cm^2, Fig 2b) than when using DL-camphorquinone (e.g. 17.5 J/cm^2 for 5% w/w composition, Fig. 2a). This result was expected because DL-camphorquinone is usually used in combination with amines as a part of a photoinitiator system rather as a stand-alone photoinitiator [27]. Furthermore, when using HHEPMP as photoinitiator, good pattern definitions could be achieved at very low concentrations (0.1 % w/w) using low laser fluences (~29 mJ/cm^2) and moderate number of laser pulses (>40) (Fig. 2b). Moreover, for HHEPMP concentrations above 0.1 % w/w, the obtained stripes were too wide (more than

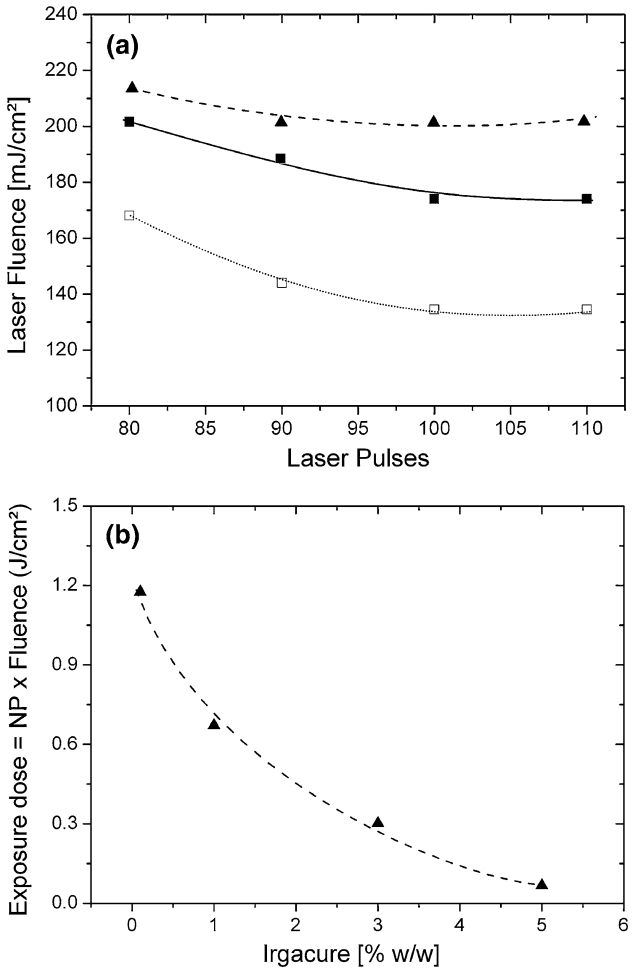

Fig. 2 **a** Laser processing conditions necessary to crosslink the photo-reactive mixture with 5 % w/w of DL-camphorquinone and 600 MW-PEGDMA. The lines presented are just to guide the eye; *Solid-line* optimum exposure conditions; *lower dashed-line* photo polymerization threshold; *upper dashed-line* upper exposure limit. **b** Exposure doses necessary to produce crosslinking at different concentrations of HHEPMP (Irgacure 2959) and 600 MW-PEGDMA (the *lines* are only to guide the eyes)

40 μm width) or no hydrogel free space area between structures was visible. This was the case even when the exposure dose was close to the lower photocrosslinking threshold. Particularly, when using high laser intensities at HHEPMP concentrations larger than 2 % w/w, the width of the PEGDMA stripes could not be controlled. As shown in Fig. 2b, the exposure dose necessary to photocrosslink the reactive PEGDMA mixture varied from 1.18 to 0.07 J/cm^2 for concentrations of HHEPMP between 0.1 and 5% w/w, respectively. This behaviour can be explained by the high reactivity and light absorptivity of the photoinitiator at a wavelength of 355 nm. This allows fast propagation of the photocrosslinking chain reaction but if not controlled can render to low definition microstructures. Thus, only the photoreactive mixture with a low content of HHEPMP could be used in a controlled way to produce micropatterns of good quality on the selected polymer prelayer.

Concerning adhesion of the photopolymerizable hydrogels fabricated either with HHEPMP or on DL-camphorquinone on PEMA, it could be noted that shorter post-irradiation heating times were required to improve adhesion of the hydrogel patterns for HHEPMP (see Table 1). Taking into account that the HHEPMP is more sensitive to UV radiation at 355 nm than DL-camphorquinone, a larger number of free radicals could be produced during the irradiation process, even at low concentrations. In consequence, some of the left over radicals can interact with the underlying polymer layer in a shorter time, thus improving adhesion. Furthermore, for both photoinitiators, it was observed that hydrophilicity is the most significant parameter influencing adhesion of the PEGDMA-microstructures. Thus, for the most hydrophobic layer (POMA) the combined effect of dewetting and the scanty polar groups available to form hydrogen bonds or other physical interaction with the ether groups of the PEGDMA chains produced non uniform micropatterns and poor adhesion to the substrate.

Another important parameter that affects the quality of the PEGDMA micropatterns is the thickness of photoreactive layer applied [28]. It was observed that irradiating at 29 mJ/cm^2 with 40 pulses (total exposure dose 1.18 J/cm^2) a mixture with 0.1 % of HHEPMP with a thickness of 125 μm gave the best results (Fig. 3a). A thicker layer of reactive mixture (200–500 μm), at the same irradiation conditions, delivered taller stripes or pillars (with an estimated height >15 μm, similar to the ones depicted in Fig. 3b) which collapsed and deformed easily in their swollen state due to their mechanical compliance (Fig. 3) [29, 30]. Furthermore, irradiation at higher exposure doses through the MLAs (either using the cylindrical or the spherical geometry) produced taller but not thicker structures or pillars when tested at fixed film thickness of 125 μm and initiator concentration of 0.1 % of HHEPMP.

Also, the geometry of the MLA influenced the exposure dose necessary to carry out photocrosslinking of the reactive mixtures. At a fixed photoinitiator concentration (e.g. 5 % DL-camphorquinone) and a fixed reactive layer thickness (e.g. 125 μm), lower exposure doses were needed to photocrosslink pillars than line structures. For example, using the spherical MLA at the same concentration of photoinitiator and layer thickness, a exposure dose of 13.4 J/cm^2 was necessary to produce the pillar hydrogel structures, while using the cylindrical MLA to produce the line-structures, the exposure dose was 17.4 J/cm^2 ($\sim$30 % higher). This effect can be explained by the shape of the lenses, since in the spherical MLA the laser energy is focused in smaller area.

By horizontally translating or rotating the sample and sequential irradiation, several geometries of PEGDA

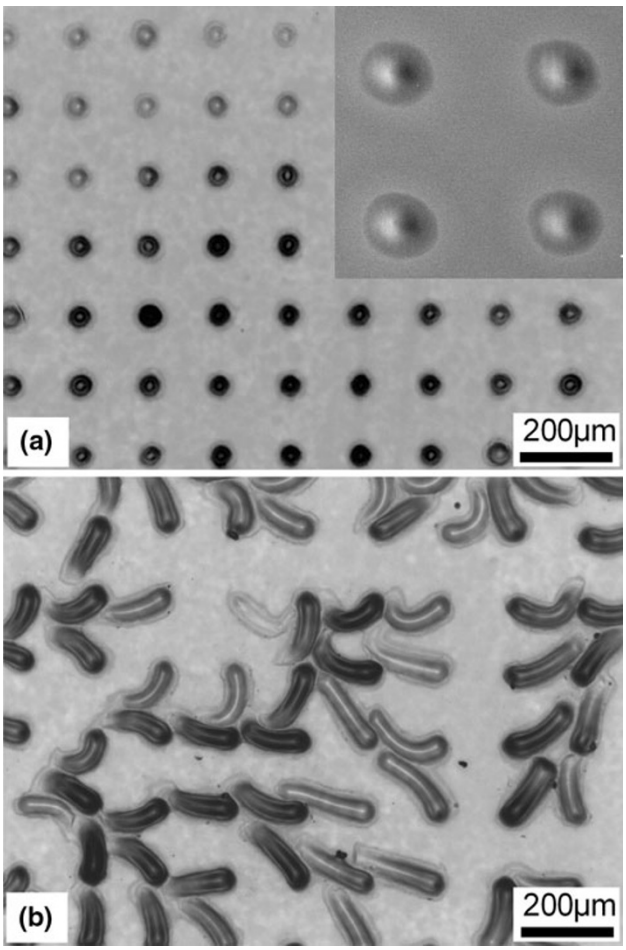

Fig. 3 Optical microscope images of dot-like micropatterns with a period of 150 μm on PEMA-coated glass irradiated with (**a**) 100 pulses at 134 mJ/cm^2 (with a total exposure dose of 13.4 J/cm^2), *inset* SEM picture and (**b**) 110 pulses also at 134 mJ/cm^2 (with a total exposure dose of 14.8 J/cm^2) on PEMA-coated glass using 5% w/w DL-camphorquinone. The photopolymerization threshold for this composition is 12.8 J/cm^2

micropatterns could be also fabricated using the 300 μm pitch (space between micro lenses in the array) cylindrical MLA. Examples of possible geometries that can be obtained are shown in Fig. 4. For instance, if the substrates are translated a distance of 50 μm and irradiated 5 times (after each translation), linear arrays with a spatial periodicity of 50 μm were obtained (Fig. 4a). Moreover, by translating the substrate different distances, patterns with different periodicity could be also fabricated (Fig. 4b). To fabricate cross-like structures, the substrates were rotated 90° between irradiation steps (Fig. 4c).

The effective width in swollen state of the optimized linear microstructures produced with HHEPMP (at 0.1 %, 40 pulses and fluence of 29 mJ/cm^2) was ~12 μm as measured from fluorescence microscopic images on microarrays with rhodamine-labelled BSA or fibronectin adsorption (Fig. 5). In dry state, the width measured from

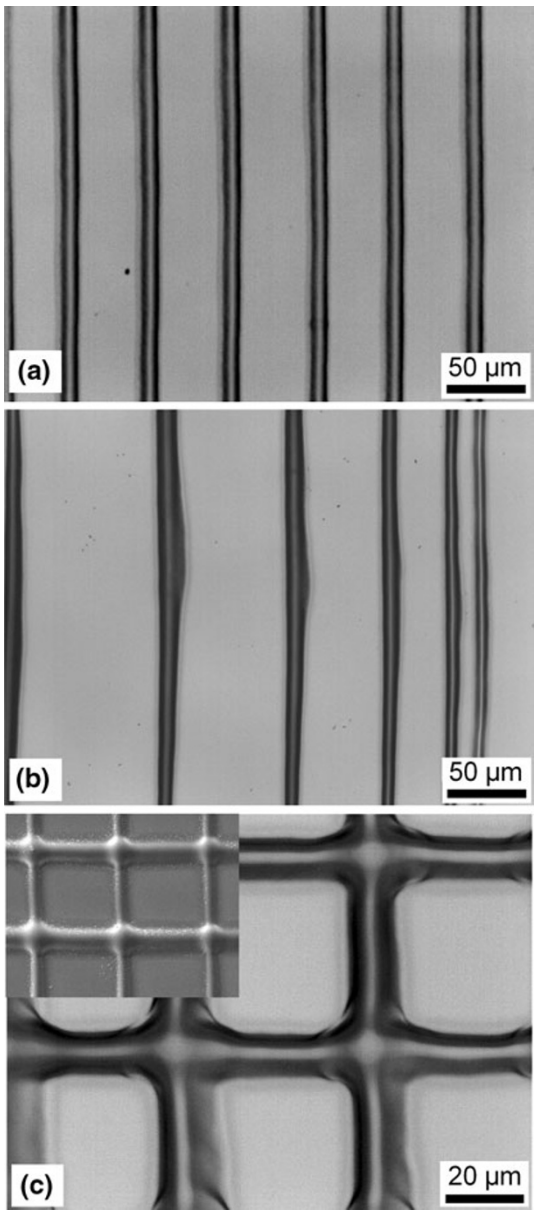

Fig. 4 Optical microscope images of: (**a**) 50 μm periodic linear micropattern on PEMA-coated glass (0.1 % w/w HHEPMP); (**b**) 20, 40, 60, 80, 100 μm periodic linear micropattern on PEMA-coated glass (0.1 % w/w HHEPMP); (**c**) 50 μm periodic cross micropattern on PEMA-coated glass (0.1 % w/w HHEPMP), *inset* SEM picture

SEM pictures was approximately ~9.0 μm. The fluorescent signal of the PEGDMA hydrogel microstructures in 2D and 3D ICLSM images (see Fig. 6) results from to residual photoinitiator (HHEPMP) trapped in the crosslinked hydrogel network. These images provided an approximation of the height of the swollen PEGDMA micropatterns which was ~10 μm (irradiated with 29 mJ/cm^2 and 40 pulses, 0.1% of HHEPMP, film thickness of 125 μm).

Adhesion of the hydrogel micropatterns to the substrate and their mechanical stability depended also on the type of

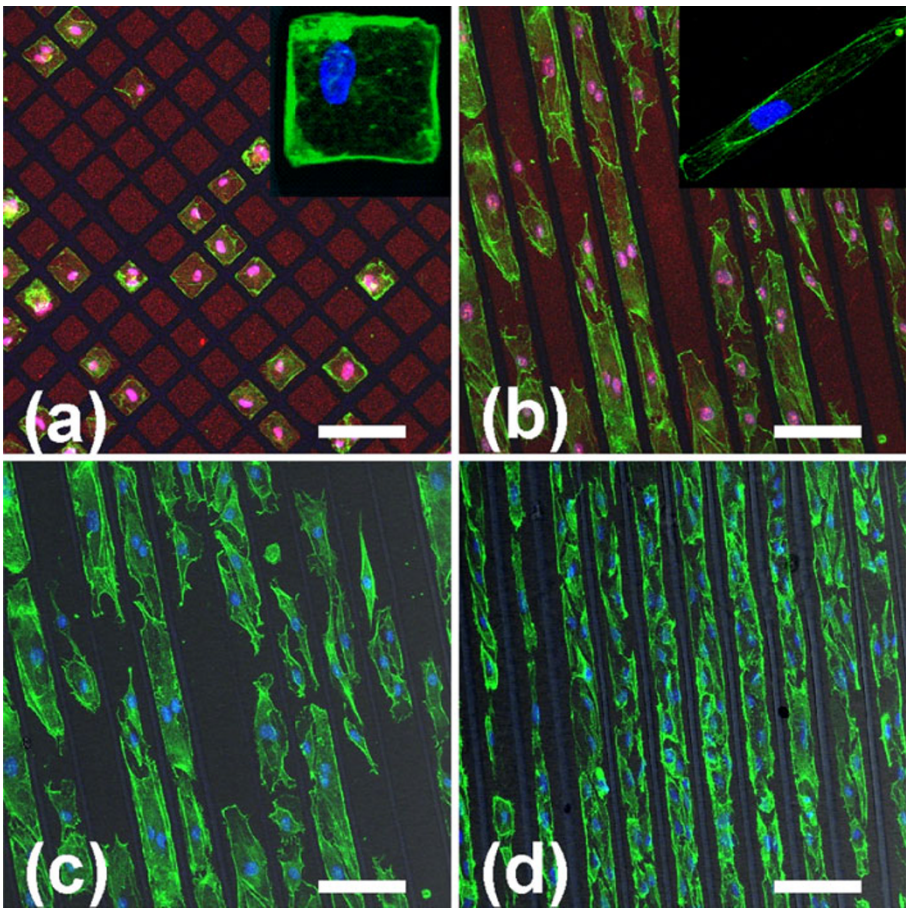

Fig. 5 Laterally patterned protein adsorption (fluorescently labelled fibronectin) and endothelial cell growth (*green*: actin cytoskeleton; magenta or *blue*: nucleus) on micropatterned PEGDMA on PEMA surfaces: (**a**) Cross and (**b–d**) linear micropatterns with spatial periods of 50 and 30 μm, respectively. The images were taken after (**a–b**) 3 h and (**c–d**) 5 days of cell culture. *Insets* in (**a**) and (**b**) show single cell close up. *Scale bars* 100 μm

the structure fabricated. Cross-like micropatterns (Figs. 4b, 5a) showed in general a better adhesion than line (Fig. 4a, b) or pillar arrays (Fig. 3a). This improvement can be due to better mechanical stability of the interconnected grid shape of the structure [23].

Finally, as a proof of concept for the potential use of the PEGDMA micropatterns for advanced in vitro assays, protein adsorption experiments and cell growth tests were performed (Fig. 5). The stability of the produced micropatterned surface was tested in dry by several wet and dry cycles at room temperature. The micropatterned surfaces can be kept dry in stable condition for several weeks, for transportation or shipping purposes, for example. Furthermore, the micropatterned surfaces could be hydrated and dried in air at room temperature from three (on PPMA and PSMA-h prelayers) to six times (on PEMA prelayer) with water showing no detachment of the microstructures.

Adsorption of fluorescent-labelled model proteins (fibronectin and albumin) showed the protein-repellent characteristics of the PEGDMA microarrays and helped to measure the effective width of the hydrogel structures in swollen state (Fig. 6a, b). Besides a slight deformation of the hydrogel micropatterns due to swelling and dehydration after a few wet-dry cycles, the cross- and linear micropatterns exhibited good adhesion and definition quality over areas of several square millimeters.

The suitability of the patterned samples for bioassays and the stability of the microstructures in terms of mechanics and anti-fouling properties were tested in cell experiments over 5 days. Because the used patterning procedure was performed under normal no sterile conditions, all the patterned substrates were first sterilized by immersion in an ethanol/water solution. During the whole cell culture period, the micropatterns showed neither indication of cell or protein adhesion nor detachment (Fig. 5c, d).

The use of these micropatterned surfaces to localize precisely protein adsorption or laterally constrain cell growth (Fig. 5a, b) was also supported in the cell adhesion experiments showing the laterally restricted adhesion of endothelial cells. These well defined and stable microstructures allow in depth investigation of cellular function under spatially restricted conditions.

Although the morphology of the surface topography can also be a factor regulating protein and cell adhesion even in protein and cell repellent surfaces [31], in this study, the chemistry of the surface seems to be the main factor controlling cell adhesion and therefore obtaining cell-repellent

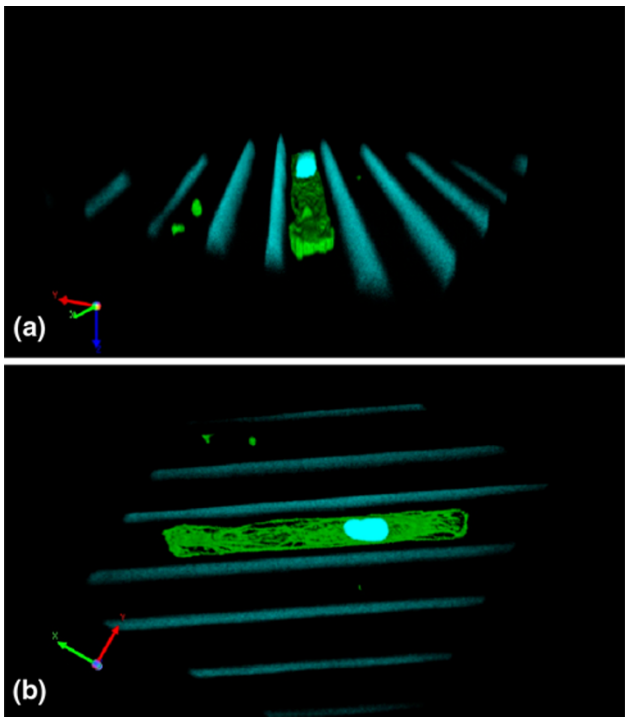

Fig. 6 Three-dimensional representation of a HUVEC in a linear micropattern with 30 μm periodicity. The fluorescence signal (due to residual photoinitiator trapped in the hydrogel network) of the PEGDMA micropattern indicates a structure height of approximately 10 μm. The patterns were produced with 40 pulses at 29 mJ/cm^2 of laser flounce (0.1 % w/w HHEPMP)

confined spaces for the cells to adhere to the polymer film that is enclosed by the PEG-structures. This can be explained due to the smooth surface of the microstructures created by MLAP, as seen in Figs. 4 and 6, and is clearly demonstrated by the square shape of an isolated HUVEC after 3 h of seeding, which is spread only in the available hydrogel free area (Fig. 5a).

From this kind of sequential experiments, valuable information could be obtained regarding cell behaviour under lateral constraints. This includes high resolution analysis of intracellular structures like the actin cytoskeleton as demonstrated in Fig. 6, where a three-dimensional representation of a single cell delimited by the PEGDMA hydrogel micropattern is depicted, indicating a well-defined restriction of cell morphology and its impact in the actin cytoskeleton.

4 Conclusions

A flexible, large area laser-assisted method to fabricate protein- and cell-repellent hydrogel patterns was presented. This procedure uses commercially available UV cross-linkable PEGDMA hydrogel and maleic anhydride copolymers layers as a biofunctional background. From the four different biofunctional prelayers tested, the PEMA copolymer permitted to improve adhesion of the hydrogel microstructures.

Several parameters affecting the micropatterning procedure could be identified including the type and quantity of photoinitiator, post- and pre-irradiation heating as well as laser intensity and pulse number (exposure dose). The photoinitiator 2-hydroxy-1-[4-(2-hydroxyethoxy)phenyl]-2-methyl-1-propane showed a higher reactivity than DL-camphorquinone at a wavelength of 355 nm, allowing micropattern fabrication at very low photoinitiator concentrations and low laser exposure doses. Well defined microdomains delimited by the anti-fouling PEGDMA micropatterns were demonstrated by protein adsorption and cell adhesion experiments. The potential use of this method to study cell-surface anchorage in restricted domains was also proved. The produced micropatterned surfaces showed good stability in normal cell culture conditions over a period up to 5 days. This procedure might be suitable for use in medium scale bioassay studies and can be used for patterning of other hydrophilic biofunctional surfaces.

Acknowledgments This work was financially supported by the Fraunhofer-Gesellschaft under Grant No. Attract 692174. H. Perez wishes to thank the Deutscher Akademischer Austausch Dienst (DAAD) for financial support.

References

1. Revzin A, Tompkins RG, Toner M (2003) Langmuir 19:9855–9862
2. Schoichet MS, Hubbell JA (1998) In: Polymers for tissue engineering. VSP, Zeist
3. Kisaalita WS (2010) 3D cell-based biosensors in drug discovery programs. CRC Press, New York
4. Hahn MS, Miller JS, West JL (2006) Adv Mater 18:2674–2684
5. Wosnick JH, Shoichet MS (2007) 3D chemical patterning of transparent hydrogels. Chem Mater 20:55–60
6. Arcaute K, Mann B, Wycker R (2010) Acta Biomater 6:1047–1054
7. Tang L, Min J, Lee EC, Kim JS, Lee NY (2010) Biomed Microdevices 12:13–21
8. Suh KY, Seong J, Khademhosseini A, Laibinis PE, Langer R (2004) Biomater 25:557–563
9. Bhadriraju K, Liu WF, Gray DS, Chen CS (2007) BioMEMS and biomedical technology, chap 3. Springer, Berlin, pp 325–343
10. Moon JJ, Hahn MS, Kim I, Nsiah BA, West JL (2009) Tissue Eng Part A 15:579–585
11. Kim DN, Lee W (2009) J Chem Tech Biotech 84:279–284
12. Yu T, Ober CK (2003) Biomacromol 4:1126–1131
13. Colpo P, Ruiz A, Ceriotti L, Rossi F (2010) Adv Biochem Eng/Bio Tech 117:109–130

14. Falconnet D, Csucs G, Grandin HM, Textor M (2006) Biomaterials 27:3044
15. Castel D, Pivatal A, Debily MA, Gridol X (2006) Drug Discovery Today 11:616–622
16. Sun JG, Tang J, Ding JD (2009) Chin Sci Bull 54:3154–3159
17. Harris JH (1993) Poly(ethylene glycol) chemistry: biotechnical and biomedical applications. Plenum, New York
18. Nguyen K, West JL (2002) Biomaterials 23:4307–4314
19. Xu W, Luikart AM, Sims CE, Allbritton NL (2010) Anal Bioanal Chem 397:3377–3385
20. Sun JG, Tang J, Ding JD et al (2009) Chin Sci Bull 54:3154–3159
21. Kim DN, Park D, Koh WG (2009) J Ind Eng Chem 15:214–128
22. Stratakis E, Rannella A, Farsari M, Fotakis C (2009) Prog Quantum Electron 33:127
23. Yuan D, Lasagni AF, Shao P, Das P (2008) Virtual Phys Prototyping 3:221–229
24. Perl A, Reinhouldt DN, Huskens J (2009) Adv Mater 21:2257–2268
25. Herklotz M, Werner C, Pompe T (2009) Biomaterials 30:35–44
26. Pompe T, Zschoche S, Herold N, Salchert K, Gouzy MF, Sperling C, Werner C (2003) Biomacromolecules 4:1072–1079
27. Jakubiak J, Allonas X, Fouassier JP (2003) 44:5219–5226
28. Arcaute K, Mann BK, Wicker RB (2006) Ann Biomed Eng 34:1429–1441
29. Jhaveri SJ et al (2009) Chem Mater 21:2003–2006
30. Padmavathi NCh, Chatterji PR (1996) Macromolecules 29:1976–1979
31. Schulte VA, Diez M, Möller M, Lensen MC (2009) Biomacromolecules 10:2795–2801